Oxygen Reduction on Platinum Low-Index Single-Crystal Surfaces in Alkaline Solution: Rotating Ring Disk Pt(hkl) Studies

ARTICLE *in* THE JOURNAL OF PHYSICAL CHEMISTRY · APRIL 1996

Impact Factor: 2.78 · DOI: 10.1021/jp9533382

2 AUTHORS, INCLUDING:

Philip N Ross
University of California, Berkeley
360 PUBLICATIONS **21,340** CITATIONS

Oxygen Reduction on Platinum Low-Index Single-Crystal Surfaces in Alkaline Solution: Rotating Ring Disk$_{Pt(hkl)}$ Studies

Nenad M. Marković,* Hubert A. Gasteiger,† and Philip N. Ross (Jr.)

Materials Sciences Division, Lawrence Berkeley Laboratory, University of California, Berkeley, California 94720

Received: November 13, 1995[⊗]

The first results of a study of the oxygen reduction reaction on a rotating ring−disk electrode using single-crystal Pt disk electrodes in alkaline solution are presented. The order of activity of Pt(*hkl*) in 0.1M KOH increased in the sequence (100) < (110) < (111) for both oxygen and peroxide reduction. These differences are attributed to the structure sensitivity of hydroxyl anion (OH^-) adsorption on Pt(*hkl*) and its inhibiting (site blocking) effect on oxygen kinetics. Two different types of OH_{ads} occur on Pt(100) and Pt(110), a reversible OH_{rv}, and an irreversible OH_{ir}, while only the reversible form is formed on Pt(111). Very small fluxes ($I_R/N \ll 0.01I_D$) of peroxide were detected at the ring at potentials where the surfaces have only the reversible form of OH_{ads}. More peroxide ($I_R/N < 0.03I_D$) was found with the Pt(100) and Pt(110)surfaces in the potential region where irreversible adsorption occurs. The mechanism of O_2 reduction was also affected by adsorbed hydrogen with increased formation of peroxide ions in this potential region; correspondingly, adsorbed hydrogen was found to have an inhibiting effect on peroxide reduction, the effect decreasing in the order (111) > (100) ≫ (110).

1. Introduction

Substantial interest in electrochemical energy conversion, particularly in fuel cells, has generated vigorous investigation of the oxygen reduction reaction (ORR) on a wide range of materials in a variety of aqueous electrolytes. Of the many surfaces examined, polycrystalline platinum is of particular interest since it is among the most active surfaces for oxygen reduction in both acid and alkaline electrolytes, while other metals or macrocyclic compounds are active in only one range of pH. Based on observations relating the kinetics of oxygen reduction at room temperature to experimental variables such as oxygen partial pressure, pH, the state of the surface (oxidized *vs* reduced), and the anion in the supporting electrolyte, a number of theories have been proposed concerning the mechanism of oxygen reduction on polycrystalline Pt.[1−3] Although the last 15 years have witnessed substantial advances in our knowledge of the electrochemistry of Pt single crystal surfaces, the dependence of the kinetics of the ORR as a function of the platinum surface geometry is still unresolved.[4−8] The principal problem in the investigation of the mechanism and kinetics of a ORR on well-defined platinum single crystals was a clean assembling of the rotating ring-disk electrode (RRDE) with the platinum single crystals in the disk configuration (RRD$_{Pt(hkl)}$E). Recently, however, we reported a new experimental method which allows fast and clean transfer of flame-annealed platinum single crystals into a true RRDE configuration.[4] This important development enabled us to control and measure independently the mass flux of electroactive species at single-crystal electrode surfaces in the study of the electrodeposition (both over and underpotential) of copper on Pt (111),[9] adsorption of anions,[10] oxidation/evolution of molecular hydrogen,[11] and the reduction of oxygen on platinum single-crystal electrodes (RRD$_{Pt(hkl)}$E).[4]

In our previous RRD$_{Pt(hkl)}$E study of the ORR in 0.05 M sulfuric acid, the kinetics were strongly sensitive to the crystallographic orientation of the platinum disk electrode. We proposed that the structural sensitivity is correlated with the state and the coverage of adsorbed (bi)sulfate anions on Pt(*hkl*).[4] Although this measurement provided a new insight on the effects of (bi)sulfate adsorption on the kinetics of the ORR, the mechanism of oxygen reduction remains uncertain.

The present study was undertaken to determine the role of adsorbed oxygen-containing species, such as OH_{ads}, in the ORR kinetics. We will report an examination of O_2 reduction kinetics on RRD$_{Pt(hkl)}$E in 0.1M KOH, employing the same procedures used in our recent detailed study in acid electrolyte.[4] In KOH, OH_{ads} can be formed simply by anion adsorption, whereas in acid electrolyte it can only be formed by water splitting. The comparison in ORR kinetics between the different platinum single crystals at these two pHs shed considerable light on the surface chemistry of adsorbed OH_{ads} species on platinum surfaces.

2. Experimental Section

The preparation, pretreatment, and assembling of the of RRD$_{Pt(hkl)}$E was fully described in our previous paper.[4] Briefly summarized, following flame annealing and cooling in hydrogen,[12] cylindrical single-crystal samples were mounted into a rotating ring−disk arbor.[13] The electrodes were immersed into either pure 0.1 M KOH (J. T. Baker Reagent) or in 0.1 M KOH containing hydrogen peroxide (Merck Suprapure) under potential control at 0.2 V; in this paper all potentials are given against the reversible hydrogen electrode (RHE). The ring was potentiostated at 1.15 V, where peroxide oxidation occurred under diffusion control. The measured collection efficiency, *N*, for our RRDE geometry is 0.22 (±5%). The geometrical surface area of the disk electrode was 0.283 cm^2. All voltammograms were recorded at 50 mV/s at room temperature, ≈25 °C.

3. Results

3.1. Cyclic Voltammetry of Pt(*hkl*) in 0.1 M KOH. Comparison of the cyclic voltammograms of Pt(*hkl*) electrodes

* To whom correspondence should be addressed: Lawrence Berkeley Laboratory, Mail Stop 2-100, 1 Cyclotron Road, Berkeley, CA 94720. Phone: (510)-486-4793. FAX: (510)-486-5530.

† Current address: Abt. für Oberflächenchemie und Katalyse, Universität Ulm, D-89069 Ulm, Germany. Phone: (731)-502-2901. FAX: (49)-731-502-5452.

⊗ Abstract published in *Advance ACS Abstracts,* March 15, 1996.

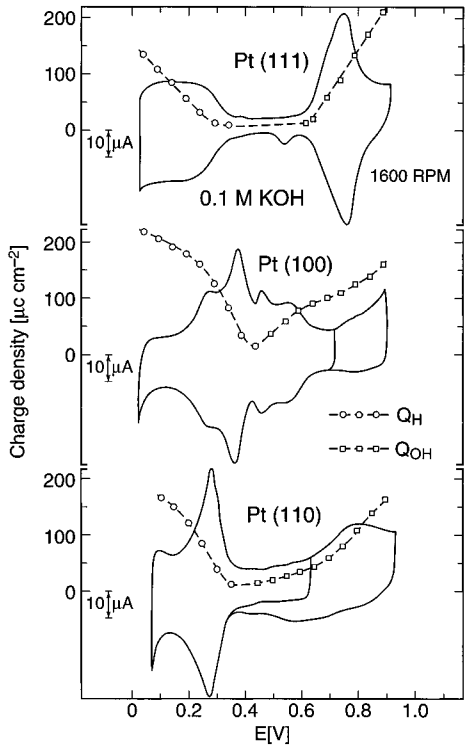

Figure 1. Cyclic voltammograms of Pt(*hkl*) disk electrode in the $RRD_{Pt(hkl)}E$ configuration in oxygen-free 0.1 M KOH and plots of the charge associated with the hydrogen and hydroxyl adsorption at 25 °C and 1600 rpm.

in oxygen-free 0.1 M KOH, Figure 1, with those in the literature[14−16] clearly demonstrates the high quality of platinum single crystals in the $RRD_{Pt(hkl)}E$ configuration. Voltammograms recorded at 0 rpm (not shown) and 1600 rpm were essentially identical, confirming that electrode assembly and the electrolyte solution were extremely clean. Figure 1 also displays plots of charges associated with both hydrogen adsorption (Q_H) and the adsorption of oxygen-containing species (Q_{OH}) on Pt(*hkl*) as a function of the electrode potential (E). In making these plots, we have associated particular regions of pseudocapacitance specifically to hydrogen adsorption or to adsorption of OH_{ads} (*i.e.,* oxygen-containing species) based on our interpretation of the voltammetry. The justification for this is discussed in a later section of the paper. There is no consensus in the literature at this time about the separation of these charges for Pt(*hkl*) electrodes in KOH.

The accuracy of the charge integration from the voltammograms of Figure 1 is primarily dependent upon two sources of possible error. One involves the method of correction for the double-layer capacitance, and the other, with the exception of the Pt(111) plane, involves uncertainty in the deconvolution of the Coulumbic charge associated with the hydrogen adsorption from the charge corresponding to the adsorption of oxygen-containing species; for simplicity we shall call this species OH_{ads}. In this work, the capacitance of the Pt(*hkl*)−solution interface was determined from the Pt(111) curve by assuming that the current in the potential region $0.35 < E < 0.65$ V is indicative of "true" double layer charging current. The numerical value extrapolated from the "double-layer" of Pt(111) (*ca.* 80 μF/cm^2) is higher than that for the double-layer capacitance of other metal surfaces such as Au(111)[17−19] (*ca.* 20 μF/cm^2). Although the reason for this difference is not clear, one might hypothesize that the high capacitance is due to the concomitant initial adsorption of OH_{ads} which essentially increases the expected double layer capacitance. The procedure for deconvoluting Q_H from Q_{OH} on Pt(100) and Pt(110) was trial-and-error curve

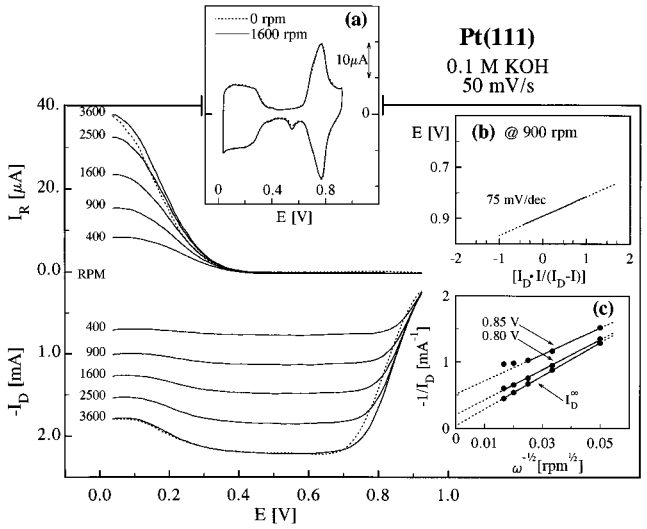

Figure 2. Disk (I_D) and ring (I_R) currents during oxygen reduction on Pt(111) in 0.1 M KOH at a sweep rate of 50 mV/s (ring potential = 1.15 V): (—) positive going sweeps; (− − −) negative going sweep at 3600 rpm. (a) Cyclic voltammetry of Pt(111) in the RRDE assembly in oxygen-free electrolyte with and without rotation; (b) Tafel plot at 900 rpm; (c) Levich plot at various electrode potentials.

fitting of the voltammetry curves such that the charge from integrating the current on the positive going sweep from ($0.05 > E > 0.5$ V) gives the number of coulombs required to remove a monolayer of adsorbed hydrogen adatoms on these two surfaces. The theoretical charge for monolayer adsorption with one-electron transfer per surface atom was based on the surface atomic density of the unreconstructed (1 × 1) geometry rather than reconstructed surfaces because our recent surface X-ray scattering (SXS) studies confirmed (1 × 1) structure of the Pt-(111) (1.5 x 10^{15} atoms/cm^2) and Pt(100) (1.3 x 10^{15} atoms/cm^2) single crystals in contact with several electrolytes.[20,21]

3.2. Oxygen Reduction on Pt(*hkl*). 3.2.1. Pt(111). Ring−disk measurements recorded on platinum low-index single crystals in O_2-saturated 0.1 M KOH are shown in Figures 2−4. In all experiments the ring was potentiostated at 1.15 V, where oxidation of peroxide arriving at the ring is under diffusion control. A characteristic feature for all three platinum single crystals is that the kinetics of O_2 reduction are different under different sweep directions; this is also a characteristic feature of polycrystalline Pt.[1] Following the interpretation of this hysteresis for polycrystalline Pt, the potentiodynamic curves recorded in the positive sweep direction represent O_2 reduction on an essentially oxide-free surface while during the negative-going sweep the reaction occurs on partially oxidized surfaces. We will be more precise about the definition of "oxide" in the Discussion section.

Polarization curves for O_2 reduction on the Pt(111) electrode are presented in Figure 2. Starting at ≈0.9 V and sweeping the disk potential negatively across the region of OH_{ads} adsorption on this surface, the O_2 reduction is under combined kinetic and diffusion control. As the disk potential approaches the double layer region, well-defined diffusion limiting currents were observed, indicating O_2 reduction is purely controlled by mass transport. Throughout the potential region between 0.8 and 0.925 V, the corresponding ring currents were a very small fraction of the disk currents ($I_r/N < 0.01 I_d$), implying that even though the surface is highly covered by OH_{ads}, *e.g.*, ≈0.5 ML at 0.8 V from Figure 1, oxygen reduction proceeds almost entirely through the $4e^-$ pathway. Below 0.3 V, however, the activity of Pt(111) for O_2 reduction becomes suppressed and parallels with the onset of adsorption of hydrogen on Pt(111);

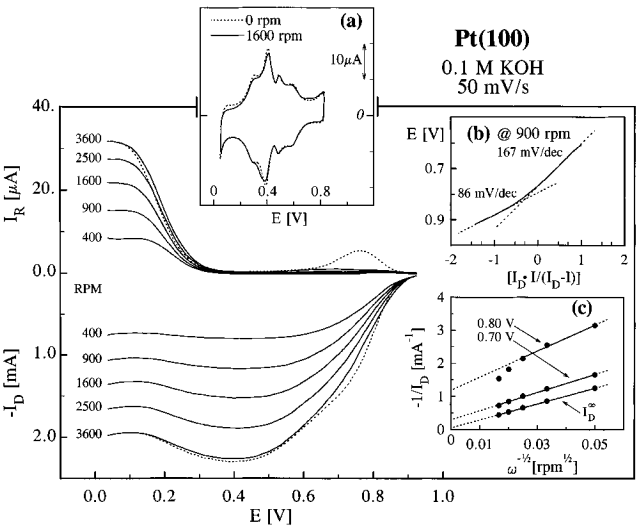

Figure 3. Disk (I_D) and ring (I_R) currents during oxygen reduction on Pt(100) in 0.1 M KOH at a sweep rate of 50 mV/s (ring potential = 1.15 V): (—) positive going sweeps; (– – –) negative going sweep at 3600 rpm. (a) Cyclic voltammetry of Pt(100) in the RRDE assembly in oxygen-free electrolyte with and without rotation; (b) Tafel plot at 900 rpm; (c) Levich plot at various electrode potentials.

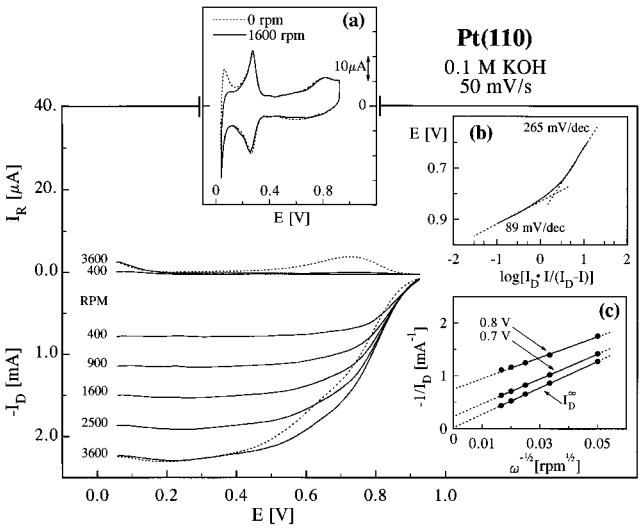

Figure 4. Disk (I_D) and ring (I_R) currents during oxygen reduction on Pt(110) in 0.1 M KOH at a sweep rate of 50 mV/s (ring potential = 1.15 V): (—) positive going sweeps; (– – –) negative going sweep at 3600 rpm. (a) Cyclic voltammetry of Pt(110) in the RRDE assembly in oxygen-free electrolyte with and without rotation; (b) Tafel plot at 900 rpm; (c) Levich plot at various electrode potentials.

see Figure 1. The change in the surface catalytic activity from $4e^-$ reduction on the hydrogen-free surface to $3.4e^-$ reduction on the surface fully covered with hydrogen adatoms is mirrored with the appearance of peroxide oxidation currents on the ring electrode. A similar effect of adsorbed hydrogen on peroxide formation on Pt(111) was observed in acid solution.[4] There, however, the formation of peroxide was quantitative to the extent that oxygen reduction in the hydrogen region on Pt(111) is a two-electron reduction, underlined by the fact that solution phase peroxide could not be reduced in this potential region.

3.2.2. Pt(100). Figure 3 shows that the potential region for combined kinetic−diffusion control for O_2 reduction is markedly extended on Pt(100). In contrast, the true diffusion limiting currents for O_2 reduction were observed in a very narrow potential range (*ca.* 0.2 V) and at high overpotential, only below 0.5 V. As the disk potential is swept positively across the potential in which the transition in the slope of the Q_{OH} *vs* E occurs (≈0.75 V in Figure 2b), the buildup of irreversibly adsorbed OH finally leads to the formation of hydrogen peroxide after the sweep reversal, as can be deduced from the increase of the ring current ($I_r/N \approx 0.03 I_d$). The reason why no peroxide formation can be observed during the positive going sweep is related to both the irreversibility of oxide formation above ≈0.8 V (see Figure 2b) and the time delay in adjusting an equilibrium state for the oxygen reduction reaction at the rather fast sweep rate of 50 mV/s. As we discuss further below, we interpret this transition in the Q_{OH} slope as a transition in the nature of OH_{ads}, namely from a reversible to an irreversible or "oxide" species, and these two different species have different effects on the ORR pathway. As with Pt(111) above, the increase in the surface coverage by hydrogen adatoms below 0.3 V clearly results in reduction of the diffusion limiting currents (from a $4e^-$ reduction to ≈$3.5e^-$ reduction), and at the same time an increase in the ring currents for HO_2^- oxidation, implying that adsorbed hydrogen increases HO_2^- production, as was found in acid electrolytes.[4]

3.2.3. Pt(110). Polarization curves for O_2 reduction on Pt-(110) exhibit quite similar behavior with results reported in the literature for polycrystalline platinum electrodes.[1] The hysteresis in the current between the anodic and cathodic sweeps was the largest on this surface. Like the (100) surface, there was a potential window near 0.7 V where peroxide is produced on the cathodic sweep, which appears to be associated with transition in the slope of the Q_{OH} curve in Figure 1, *i.e.*, the transition in the nature of OH_{ads} from reversible to irreversible or "oxide" species.

3.2.4. Kinetic Analysis. All kinetic analysis was done with current−potential curves recorded on the positive going (anodic) sweep. Inserts (c) in Figures 2−4 display Levich plots for various potentials; I^{-1} *vs* $\omega^{-0.5}$ yields straight lines with intercepts corresponding to the kinetic currents, I_k. Note that at the same potential (*e.g.*, 0.8 V), $I_k(111) > I_k(110) > I_k(100)$ which gives the order of absolute kinetic activity of the three surfaces. The slope of the straight lines, the so called B factor, allows one to assess the number of electrons involved in the oxygen reduction reaction. The experimental value of Bc_0, 4.00×10^{-2} (±1%) mA $rpm^{-0.5}$ evaluated from Figures 2−4 agrees well with the theoretical value, 3.99×10^{-2} mA $rpm^{-0.5}$, for a $4e^-$ reduction using literature data for O_2 solubility, $c_o = 1.21 \times 10^{-3}$ mol/L[22]), viscosity ($\nu = 1.008 \times 10^{-2}$ cm^2/s[23]) and oxygen diffusivity, and $D = 1.86 \times 10-5$ cm^2/s.[22]

The inserts (b) of Figures 2−4 show Tafel plots of mass-transport corrected currents at Pt(*hkl*) surfaces. Figure 2 displays that on Pt(111) a single linear Tafel slope (≈75 mV/decade) was obtained in the entire potential region. The absence of a transition in the Tafel slope on Pt(111) anywhere in the potential region where oxygen reduction is under mixed activation and mass transfer control, $E > 0.75$ V, appears to be related to the single slope of Q_{OH} *vs* E curve, shown in Figure 2a. In contrast, the Tafel slopes on Pt(100) and Pt(110) increased monotonically with the overpotential. Depending on the fitting method, *i.e.*, the method of drawing the tangent through the points of what appear to be continuous curves, one might extrapolate any Tafel slope between *ca.* 60 to 250 mV/decade. In our case, we somewhat arbitrarily fitted the curves with two slopes: a low Tafel slope (86 mV/decade on Pt(100) and 89 mV/decade on Pt(110)) obtained by fitting a tangent to the polarization curve at low overpotentials; *i.e.*, $0.85 < E < 0.9$ V where $I/I_d \approx 0.05$; and a high Tafel slope (167 mV/decade on Pt(100) and 265 mV/decade on Pt(110)) from the tangent fitted through points

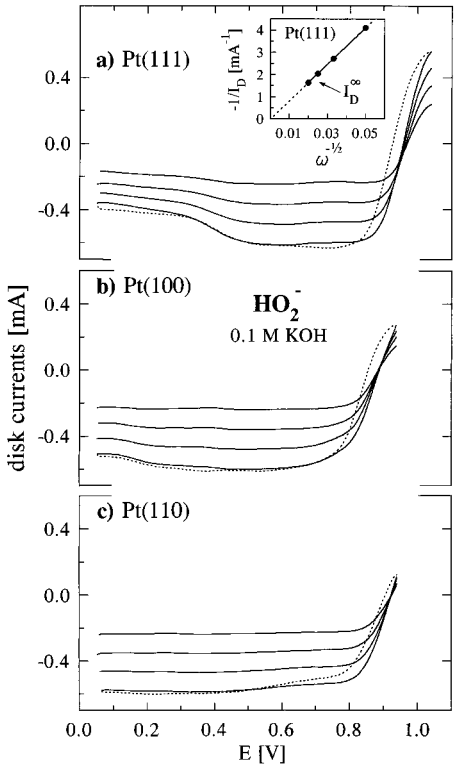

Figure 5. Polarization curves for reduction of 1.2×10^{-3} HO_2^- on Pt(*hkl*) in 0.1 M KOH: (—) positive-going sweeps; (— — —) negative-going sweep at 3600 rpm. Insert: Levich plot inferred from Pt(111) at 0.6 V.

on the polarization curve at high overpotentials but where the ratio between I/I_d was chosen to be close to $I/I_d \approx 0.9$, *i.e.*, close to the potential where the kinetics are not yet masked by mass transport resistance. The transition in the Tafel slopes on both Pt(110) and Pt(100) at 0.8 V appears to be related to the change in the slopes of the Q_{OH} vs E curves (Figure 2, b and c) and reflect changes in the nature of OH_{ads} with potential, a transition which strongly affects the ORR.

3.3. Peroxide Reduction on Pt(*hkl*). In order to fully elucidate the structural effects of Pt(*hkl*) on O_2 kinetics in alkaline solution, the HO_2^- reduction was studied on platinum single-crystal surfaces in the solution free of oxygen. To simulate the chemical environment during O_2 reduction we added peroxide to the supporting electrolyte to a concentration approximating the level of peroxide produced during the oxygen reduction, *i.e.*, the maximum level would be equal to the solubility of oxygen in the electrolyte or *ca.* 10^{-3} M. Figure 5 shows the family of polarization curves for HO_2^- reduction currents obtained on the three platinum low-index surfaces. The order of activity of Pt(*hkl*) for peroxide reduction in the potential regime where the HO_2^- reduction is under combined kinetic and diffusion control increases in the same sequence as for O_2 reduction, Pt(100) < Pt(110) < Pt(111). One should note, however, that the half-wave potentials for HO_2^- reduction curves lies well anodic (≈120 ± 5 % mV) from the half-wave potentials for O_2 reduction. This is an is important observation and indicates that if HO_2^- is formed as an intermediate on the electrode, it is immediately reduced electrochemically since the potential of oxygen reduction is negative of the region of HO_2^- stability on the platinum single-crystal surfaces. Negative of the region of combined control, the reduction of peroxide approaches the diffusion limiting current. In harmony with the interpretation of the O_2 reduction results in Figures 2−4, HO_2^- reduction is reduced below the diffusion limiting value when the potential is scanned negatively into the hydrogen adsorption region; the magnitude of the effect was in the same order as for O_2 reduction, *i.e.* Pt(111) < Pt(100) < Pt(110).

The I^{-1} *vs* $\omega^{-0.5}$ plots on Pt(*hkl*) assessed in the combined kinetic−diffusion potential region for HO_2^- reduction (not shown) are linear. At ≈0.6 V, for all three surfaces the intercept becomes zero (insert in Figure 5 is representative for all Pt(*hkl*) surfaces), implying pure mass transfer control. The B value derived from the Levich slope of the linear curve is $Bc_0 \approx 1.2 \times 10^{-2}$ mA rpm$^{-0.5}$. This value is the same as the theoretical value calculated for the 2e$^-$ reduction using the literature data for viscosity ($\nu = 1.009 \times 10^{-2}$ cm^2 s^{-1} [23]) and HO_2^- diffusivity, $D = 8.75 \times 10^{-6}$ cm^2 s^{-1}.[24]

4. Discussion

The cyclic voltammetry on different single-crystal surfaces in alkaline solution we have reported here clearly shows that the elimination of surface heterogeneity and the enhancement of the resolution in the voltammetry that results from single-crystal geometry give a new insight into complex processes associated with the adsorption of hydrogen and hydroxyl ions. This is especially true for Pt(111) and Pt(100) surfaces, where the homogeneity of the surface results in an increase in the fine structures not evident on an atomically rough surface, such as a polycrystalline platinum electrode. We present here an interpretation of the kinetics of the ORR on the different Pt(*hkl*) surfaces based on the supposition, which we shall substantiate below, that the differences arise mainly from the structure-sensitive adsorption of both hydrogen and hydroxyl ions, both impeding the reaction; *i.e.*, they are spectator species and not intermediates.

4.1. Hydroxyl Adsorption on Pt(*hkl*). 4.1.1. Pt(111). The interpretation of the voltammetry of Pt(111) in various electrolytes has been the subject of considerable controversy since 1980. Overviews with somewhat different perspectives can be found in refs 25−27. A consensus in interpretation appears to be emerging with respect to the voltammetry of the (111) surface in sulfuric acid. The current−potential curve of Pt(111) in 0.1 M KOH gives a distinctive voltammogram with the broad nearly flat hydrogen adsorption peak between 0.05 and 0.35 V, and the so-called "anomalous" peak at 0.6−0.85 V, as shown in Figure 1. The total charge for the adsorbed hydrogen on Pt(111) is *ca.* 150 μC/cm^2, close to the 160 μC/cm^2 obtained in acid solution. Our group has recently demonstrated using in situ surface X-ray scattering[21] that the "anomalous" feature recorded in perchloric acid is not "strongly" adsorbed hydrogen; together with other electrochemical methods we were recently able to attribute this pseudocapacitance to the formation/adsorption of hydroxyl species.[10] Since the anomalous feature occurs at the same potential with respect to the RHE in both $HClO_4$ and KOH,[28] the anomalous pseudocapacitive feature in 0.1 M KOH is most likely related to the adsorption of hydroxyl species,[15,16] in this case simply given by

$$OH^- \leftrightarrow OH_{ads}^{(1-\gamma)-} + \gamma e^- \qquad (1)$$

where γ denotes the electrosorption valency for the adsorbed OH. The anodic/cathodic symmetry of the voltammetry, and the coulometry, indicate that this anion adsorption process is highly reversible on Pt(111) up to the highest potentials used in this work, 0.925 V, for simplicity we shall call this species OH_{rv}. The $Q_{OH}-E$ curve of Pt(111) in Figure 1 shows that the total charge amounts to ≈220 μC/cm^2, which would correspond to the coverage of 0.9 monolayer assuming the OH_{ads} ion is completely discharged, $\gamma = 1$ (240 μC/cm^2 for 1e$^-$ per atom on Pt(111)-(1×1)).

4.1.2. Pt(100). Cyclic voltammetry of Pt(100) in 0.1 M KOH is shown in Figure 1; while voltammetry of this surface in KOH has been presented before,[14,16] an interpretation of the many features in the "double layer" region has only been discussed in ref 16. The main characteristic of well-ordered Pt(100) in alkaline solution is that a "true" double layer potential region does not exist on this surface. On the positive going sweep, for example, the desorption of hydrogen is immediately followed by the adsorption of oxygenated species. However, the potential at which this transition occurs is not at where it might appear to be from intuition; *i.e.*, it is not at 0.6−0.7 V, but at about 0.45 V. Following our extrapolation method for assessing the charge associated with the stripping of a monolayer of hydrogen, and assuming 208 μC/cm^2 corresponds to a full monolayer coverage, we found that H_{ads} stripping would be complete at ≈0.45 V; conversely, integrating the cathodic currents from 0.45 to 0.05 V gives approximately one monolayer of hydrogen. If the charge in the potential region between 0.45 and 0.7 V were to be assumed to be adsorbed hydrogen, the coverage would be more than 150% of a monolayer. There is no precedent for supermonolayer coverage of hydrogen on Pt surfaces. Therefore, a reversible pseudocapacitive feature recorded in the potential range $0.45 < E < 0.70$ V must be associated with the adsorption of species which are different than hydrogen. In alkaline solution an obvious candidate is hydroxyl anion adsorption; therefore, we have assigned this pseudocapacitance to the reversible adsorption of OH_{rv}, analogous to the adsorption on the (111) surface. At more positive potentials, however, *i.e.*, $0.75 < E < 0.95$ V, the observed asymmetry in current−voltage traces between positive and negative sweep directions clearly represents an irreversible state of adsorption, which we shall call OH_{ir}, hereafter. This transition also occurs on Pt(100) in acid electrolyte, and the nature of the transition was studied in considerable detail with ex situ LEED by Wagner and Ross.[29] Their interpretation of the process follows closely the seminal work by Conway and co-workers[30,31] on polycrystalline Pt, again mostly in acid electrolyte. For Pt(100) in acid, the number of Pt atoms place-exchanged was a function of the applied potential and the time, or under potentiodynamic conditions, of the potential limit and the sweep rate. The driving force for place exchange is an increase in coordination of OH ligands about the surface Pt atoms. Historically, this process has been generically called "oxide" formation, without necessarily being this specific about the details of the process or the structure of the "oxide". In this concept it is the place exchange which causes the "oxide" reduction process to become irreversible. Here in KOH, however, the transition from reversible to irreversible (Figure 1) character occurs at ca. 0.75 V at 50 mV/s corresponding to a total anodic charge of ≈165 μC/cm^2 . This charge would amount to the coverage of only ≈0.75 monolayer of completely discharged OH_{ads} ($\gamma = 1$).

4.1.3. Pt(110). The Pt(110) surface exhibits the closest to the more familiar polycrystalline surface voltammetry, with clear separation of hydrogen adsorption pseudocapacitance from other processes. Figure 1 shows that on the positive sweep stripping of a monolayer of hydrogen (147 μC/cm^2 within $0 < E < 0.35$V) is immediately followed by reversible adsorption of OH_{ir} ($0.35 < E < 0.65$), so that as on (100) there is no "true" double layer potential region on Pt(110). The reversible adsorption of OH_{rv} is followed by a reversible/irreversible transition above about 0.75 V. The amount of OH_{rv} adsorption at the transition point is significantly less than a monolayer if the OH_{rv} is completely discharged, about 100 μC/cm^2 or about 2/3 ML (147 μC/cm^2 for 1e$^-$ per atom on the Pt(110)-(1×1) surface). As

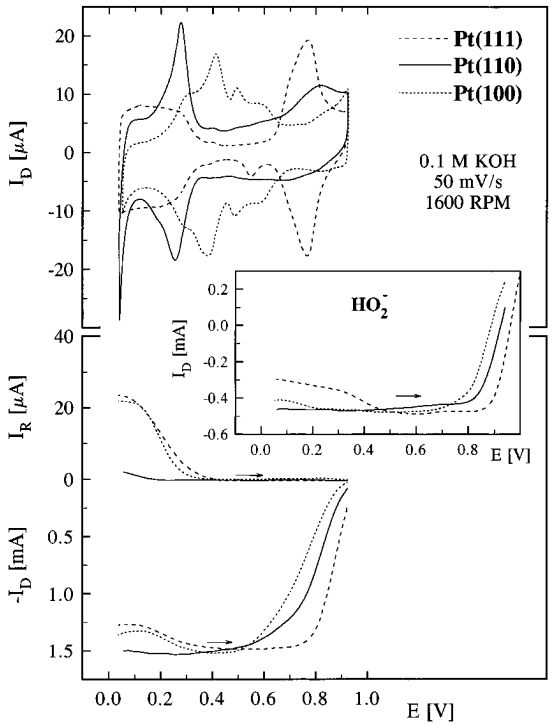

Figure 6. (Top) Cyclic voltammetry of Pt(*hkl*) in oxygen-free 0.1 M KOH electrolyte in the RRDE assembly (5th sweep). (Bottom) Disk (I_D) and ring (I_R) currents during oxygen reduction on Pt(*hkl*) (ring potential = 1.15 V). Insert: reduction of HO_2^- on Pt(*hkl*) mounted in the RRDE assembly; 01 M KOH, 50 mV/s, 1600 rpm.

with the Pt(100) surface above, we do not know for certain what physical process is associated with the reversible/irreversible transition on the (110) surface in KOH, but it is reasonable to suggest that as in acid electrolyte it is place exchange. Upon reduction of such a phase, however, no effect on the surface structure was observed on both Pt(100) and Pt(110), indicating that no structure disordering occurred on the time scale (*i.e.*, the sweep rate of 50 mV/s) and the positive potential limits of these experiments.

4.2. Effect of OH Adsorption on the Kinetics and Mechanism of O_2 Reduction. In the potential region where oxygen-containing species are present on the Pt(*hkl*) surfaces, the simplest explanation for the structural sensitivity of O_2 reduction is provided by the structure sensitive adsorption of OH_{ads} (*i.e.*, a variation in the surface coverage by both OH_{rv} and OH_{ir} species) on the different single-crystal surfaces and its inhibiting (site blocking) effect on the ORR. A close inspection of Figure 6 shows that the deviation from 4e$^-$ reduction pathway occurs in parallel with the incipient adsorption of OH_{rv}, *i.e.*, on Pt(110) this transition is observed at 0.375 V, on Pt(100) at 0.475 V and on Pt(111) at ≈0.65 V. Thus, the structure sensitivity of the ORR in the potential region of OH_{rv} adsorption in KOH would have the same origin as that in sulfuric acid, namely the structure-sensitive (reversible) adsorption of the anion in the supporting electrolyte, thereby blocking sites for the adsorption of molecular oxygen. This explanation works best for Pt(111), where there is a significant shift in the onset of OH_{rv} adsorption on this surface in comparison with the other low-index surfaces, and it is the most active surface. However, although the apparent surface coverage by adsorbed OH_{rv} on Pt(110) at ≈$E > 0.55$ V is similar, if not slightly higher, than on Pt(100), the activity of this surface for O_2 reduction is higher than on the Pt(100) surface. Either the true coverage by OH_{rv} is actually different ($\gamma < 1$ on one or both surfaces) on these surfaces or the blocking action of the OH_{rv} is different on the two surfaces. With the regards to the latter one might

note that if the adsorption of hydroxyl ion is predominantly in the "trough" positions on the (110) surface, it would leave the top sites available for the adsorption of O_2. Figure 6 also shows that in the potential region where O_2 is under combined kinetic and diffusion control on Pt(*hkl*), the activity of the surfaces for oxygen reduction decreases in the sequence (111) > (110) > (100). It is interesting that, although the reversible adsorption of hydroxyl ion, OH_{rv}, on Pt(*hkl*) suppresses the surface activity (negative shift of the half-wave potential) for O_2 reduction, it does not affect the pathway of the reaction since peroxide is not detected on the ring electrode for any of the surfaces in the potential range where the reversible form of OH_{rv} is present on the surface. Therefore, it appears that the reversibly adsorbed OH_{rv} indeed affects the ORR similarly as specifically adsorbed (bi)sulfate anions, namely in terms of a pure spectator species, blocking surface sites for the adsorption of molecular oxygen.

In contrast, irreversibly adsorbed OH_{ir}, historically termed "oxide", does change the reaction pathway (as does the adsorbed hydrogen), so the peroxide is detected at the ring when there is a significant amount of this form on the surface, as seen in the negative going sweeps from 0.925 V on (100) and (110). The reason why this does not occur during the positive going sweep is merely a time effect due to the fast sweep rate of 50 mV/s, as discussed before. One might argue that the change in the O_2 reduction mechanism should be rather correlated with the change in the surface coverage by OH_{ads} than with the nature of the OH_{ads}. However, on the positive going sweep on the (110) surface, the total coverage by OH_{ads} was at least one monolayer (if $\gamma < 1$ it would be even higher) at about 0.85 V, higher than the coverage on either of the other two surfaces at any of the potentials used here ($E < 0.925$ V), yet there was no peroxide observed. Also, no peroxide was detected on Pt(111) on the negative going sweep even though the apparent ($\gamma = 1$) coverage by OH_{ads} was nominally higher than on the (100) surface, ≈0.9 ML on Pt (111) *vs* ≈ 0.8 ML on Pt(100); the difference is that all of the 0.9 ML on (111) is reversible OH_{rv} whereas on (100) there is a significant amount of irreversible OH_{ir} (if $\gamma < 1$ for adsorption on (100), then the true coverage would actually be much higher than 0.8 ML on this surface, and we could not distinguish the two effects from these data alone). While we do not contend that the two effects can be distinguished under all conditions on all three surfaces, the weight of experimental evidence presented here favors the conclusion that reversible and irreversible OH_{ads} affects the ORR in different ways: while a reversible OH_{rv} species only effect on the initial adsorption of O_2, OH_{ir} affects both the initial adsorption of O_2 and the reaction mechanism.

Finally, we consider the issue of the Tafel slopes on the different Pt(*hkl*) surfaces. We have already pointed out that it is very difficult to discern a "true" Tafel slope from polarization curves recorded on Pt(*hkl*), with exception of Pt(111) which shows one single Tafel slope. On the contrary, on Pt (100) and Pt(110) one can extrapolate almost any Tafel slope in the range of 60−250 mV/decade, with values ranging from 60 to 120 mV/decade at low and intermediate overpotentials, similarly to what is found in the literature for O_2 reduction on a polycrystalline platinum electrode. A number of theories have been proposed to explain the transition in the Tafel slope and it is not fruitful to review them all in this paper. For our purposes here, we will focus on two the most frequently used theories. Damjanovic and Genshaw[32] attributed two slopes to a change from a Temkin to Langmuir adsorption isotherm for reaction intermediates with decreasing coverage with the first electron transfer as rate determining step. On the other hand, first Tarasevich[33] and later on Uribe et al.[34] explained this behavior as being due to a change in the surface coverage of the chemisorbed oxygen-containing species (produced by the oxidation of water in acid solution) which affect the adsorption of molecular O_2; the first charge transfer step is still rate determining. It, however, has been very difficult to obtain definitive evidence which will support either theory, since both the true nature of intermediates in the O_2 reduction have never been probed experimentally and the surface coverage of adsorbed OH_{ads} was poorly defined on a polycrystalline platinum electrode. By eliminating the surface heterogeneity with single-crystal electrodes, we obtain a clearer idea of the coverage of the surface by adsorbed OH_{ads}, gaining new insight in understanding the effect of surface coverage by OH_{ads} on the Tafel slopes. We do not claim that our analysis reported here is definitive, and it is in fact just a model, following the earlier analysis proposed by Uribe *et al.*[34]

We will proceed by accepting the hypothesis that the change in the Tafel slope implies a change in the rate determining step. The Tafel slopes at low overpotential (*ca.* $0.9 < E < 0.75$V) can be analyzed based on a very simple assumptions. First, we assume that the rate determining is the first charge transfer step, *i.e.*,

$$O_2 + e^- = O_2^- \tag{2}$$

Second, we consider that the rate of O_2 reduction at hydroxyl free Pt(*hkl*) sites increases with the overpotential according to a simple Tafel relation, *i.e.*, at 120 mV/decade of current density. We consider a simple form of single site elimination by adsorbed OH_{ads} and that the rate of O_2 reduction decreases linearly with the surface coverage by OH_{ads}. Finally, if the standard free energy of adsorption of oxygen containing species is independent of coverage, *i.e.*, if a Langmuir isotherm, is applicable, then the rate of O_2 reduction may be expressed as

$$I = nFke_{O_2}(1 - \theta_{OH_{ads}}) \exp\left(\frac{-\alpha F\eta}{RT}\right) \tag{3}$$

and corresponding Tafel relation could be found from

$$\frac{\partial \log i}{\partial \eta} = \frac{\alpha F}{2.3RT} + \frac{1}{(1 - \theta_{OH_{ads}})} \frac{\partial \theta_{OH_{ads}}}{\partial \eta} \tag{4}$$

where $\theta_{OH_{ads}}$ is the partial coverage by hydroxyl species, i, is the observed current, α is the transfer coefficient, and η is applied overpotential. If we take α to have the usual value of 0.5, then the first term corresponds to a Tafel slope of 120 mV/decade. The second term will cause the Tafel slope to vary with potential, *i.e.*, the Tafel plots are curved, when it is of the same order of magnitude as the first term, which occurs when $\theta_{OH_{ads}} > 0.5$ ML. Qualitatively, this model rationalizes the curvature of the Tafel plots for (100) and (110), since $\theta_{OH_{ads}} > 0.5$ ML for $E > 0.8$ V which is the region where the Tafel slope is between 60 and 100 mV/decade. If we assume that the presence of O_2 in solution has no effect on the coverage of OH_{ads}, and we use the Q *vs* E curves in Figure 1, we can calculate the Tafel slopes expected from this model. In the low-overpotential region where $\theta_{OH_{ads}} \approx 0.8$ ML, the calculated slopes are 63 mV/decade for (111), 83 mV/decade for (100) and 58 mV/decade for (110). These agree fairly well for the (100) and (111) surface, less so for the Pt(110), but considering the simplicity of the model, and the fact that there was some arbitrariness to the way of evaluating θ and $\partial\theta/\partial\eta$, the agreement overall is reasonable. Since in the potential region where we can obtain Tafel plots the surface is never free of OH_{ads}, the slope should be always lower than 120 mV/decade, and a

transition to a slope greater than 120 mV/decade implies a change in the rate-determining step (rds). Therefore, we conclude that the transitions in Tafel slope below about 0.8 V on (100) and (110) represent a change in the rds from eq 2. We agree with the hypothesis first presented by Tarasevich[33] that the so-called high Tafel slopes of 250−300 mV/decade on Pt (and other Pt group metals) correspond to the adsorption of molecular oxygen as the rds.

5. Conclusions

The first results of a study of the oxygen reduction reaction on a rotating ring−disk electrode using single-crystal Pt disk electrodes in alkaline solution are presented. In the potential range where O_2 reduction is under combined kinetic−diffusion control ($E > 0.75$ V) the order of activity of Pt(*hkl*) in 0.1M KOH increased in the sequence (100) < (110) < (111); the same order is observed for the reduction of HO_2^-. The shift in half-wave potential between the least active and the most active surface was *ca.* 110 mV, which is more than an order of magnitude difference in kinetic rate. These differences are attributed to the structure sensitivity of hydroxyl anion (OH^-) adsorption on Pt(*hkl*) and its inhibiting (site blocking) effect on both oxygen and HO_2^- kinetics. Two different types of OH_{ads} occur on Pt(100) and Pt(110), a reversible OH_{rv} and an irreversible OH_{ir}, while only the reversible form is formed on Pt(111). Very small fluxes ($I_R/N \ll 0.01I_D$) of peroxide were detected at the ring at potentials where the surfaces have only the reversible form of OH_{ads}. More peroxide ($I_R/N < 0.03I_D$) was found with the Pt(100) and Pt(110)surfaces in the potential region where irreversible adsorption occurs. Although it was difficult to separate the effects of coverage from the form of the adsorbate, it appears that the inhibition by the irreversible form is stronger, suggesting perhaps cooperative effects associated with a 2-D adlayer. The mechanism of O_2 reduction was also affected by adsorbed hydrogen with increased formation of HO_2^- in this potential region; correspondingly, adsorbed hydrogen was found to have an inhibiting effect on HO_2^- reduction, the effect decreasing in the order (111) > (100) ≫ (110).

Acknowledgment. We thank Lee Johnson and Frank Zucca for their invaluable help in polishing the single crystals and setting up of the experimental apparatus. This work was supported by the Assistant Secretary for Conservation and Renewable Energy, Office of Transportation Technologies, Electric and Hybrid Propulsion Division of the U.S. Department of Energy, under Contract No. DE-AC03-76SF00098.

References and Notes

(1) Tarasevich, M. R.; Sadkowski, A.; Yeager, E. Oxygen Electrochemistry. In *Kinetics and Mechanisms of Electrode Processes*; Conway, B. E., Bockris, J. O'M., Yeager, E., Khan, S. U. M., White, R. E., Eds.; Comprehensive Treatise of Electrochemistry; Plenum Press: New York, 1983; Vol. 7, pp 301−398.

(2) Kinoshita, K. *Electrochemical Oxygen Technology*; John Wiley & Sons: Inc.: New York, 1992.

(3) Sepa, D. B.; Vojnović, M. V.; Damjanović, A. *Electrochim. Acta* **1980**, *25*, 1491.

(4) Marković, N. M.; Gasteiger, H. A.; Ross, P. N. *J. Phys. Chem.* **1995**, *99*, 3411.

(5) Marković, N. M.; Adzić, R. R.; Cahan, B. D.; Yeager, E. B. *J. Electroanal. Chem.* **1994**, *377*, 249.

(6) El Kadiri, F.; Faure, R.; Durand, R. *J., Electroanal. Chem.* **1991**, *301*, 177.

(7) Abe, T.; Swain, G. M.; Sashikata, K.; Itaya, K. *J. Electroan. Chem.* **1995**, *382*, 73.

(8) Kita, H.; Gao, Y.; Ohnishi, K. *Chem. Lett.* **1994**, 73.

(9) (a)Marković, N. M.; Gasteiger, H. A.; Lucas, C.; Tidswell, I. M.; Ross, P. N. (Jr.) *Surf. Sci.* **1995**, *335*, 91. (b) Marković, N. M.; Gasteiger, H. A.; Ross, P. N. (Jr.) *Langmuir* **1995**, *11*, 4098.

(10) Gasteiger, H. A.; Marković, N. M.; Ross, P. N. (Jr.), submitted to *Langmuir*.

(11) Marković, N. M.; Gasteiger, H. A.; Sarraf, S.; Ross, P. N. *J. Phys. Chem*., in preparation.

(12) Marković, N.; Hanson, M.; McDougal, G.; Yeager, E. *J. Electroanal. Chem.* **1986**, *241*, 309.

(13) Pine Instrument Co., 101 Industrial Drive, Grove City, PA 16127.

(14) Clavilier, J.; Orts, J. M.; Feliu, J. M.; Aldaz, A. *J. Electroanal. Chem.* **1990**, *293*, 197.

(15) Wagner, F.; Ross, P. N. *J. Electroanal. Chem.* **1988**, *250*, 301.

(16) Marinković, N. S.; Marković, N. M.; Adzić, R. R. *J. Electroanal. Chem.* **1992**, *330*, 433.

(17) Hamelin, A. *J. Electroanal. Chem*. **1986**, *210*, 30.

(18) Zei, M.; Lehmpfuhl, G.; Kolb, D. *Surf. Sci.* **1989**, *221*, 23.

(19) Ross, P. N.; D'Agostino, *Electrochim. Acta* **1992**, *37*, 615.

(20) Tidswell, I. M.; Marković, N. M.; Ross, P. N. (Jr.) *Phys. Rev. Lett.* **1993**, *71* 1601.

(21) Tidswell, I. M.; Marković, N.; Ross P. N. *J. Electroanal. Chem.* **1994**, *376*, 119.

(22) Davis, R. E.; Horvath, G. L.; Tobias, C. W. *Electrochim. Acta* **1967**, *12*, 287.

(23) *CRC Handbook of Chemistry and Physics*, 66th ed.; Weast, R. C., Ed.; CRC Press: Boca Raton, FL, 1986.

(24) Zurilla, R. W.; Sen, R.; Yeager, E. *J. Electrochem. Soc.* **1965**, *112*, 469.

(25) Marković, N. M.; Tripković, A. V.; Marinković, N. S.; Adzić, R. R. Hydrogen Electrosorption and Oxidation of Formic Acid on Platinum Single-Crystal Stepped Surfaces, IR Spectroscopy of Molecules at the Solid-Solution Interface. In *Electrochemical Surface Science. Molecular Phenomena at Electrode Surfaces*; Soriaga, M. P., Ed.; ACS Symposium Series; American Chemical Society: Washington, DC, 1988; pp 497−517.

(26) Ross, P. N. *J. Chim. Phys.* **1991**, *88*, 1353.

(27) Clavilier, J.; Rodes, A.; Achi, K. El.; Zamakhchari, M. A. *J. Chim. Phys.* **1991**, *88*, 1291.

(28) Marković, N.; Ross, P. N. *J. Electroanal. Chem.* **1992**, *330*, 499.

(29) Wagner, F. T.; Ross, P. N. *Surf. Sci.* **1985**, *160*, 305.

(30) Angerstein-Kozlowska, H.; Conway, B. E.; Sharp, W. B. A. *J. Electroanal. Chem.* **1973**, *9*, 43.

(31) Conway, B. E. *Prog. Surf. Sci.* **1986**, *16*, 1.

(32) Damjanovic, A.; Genshaw, M. A. *Electrochim. Acta* **1970**, *15*, 1281.

(33) Tarasevich, M. *Elektrokhimiya*, **1973**, *9*, 578.

(34) Uribe, F. A.; Wilson, M. S.; Springrer, T. E.; Gottesfeld, S. *Proceedings of the Workshop on Structural Electrocatalysis and Oxygen Electrochemistry*; The Electrochemical Society: Pennington, NJ, 1993; Vol. 92−11, p 494.

JP9533382